

# Soft X-Ray Microscopy

Chris Jacobsen  
Department of Physics  
State University of New York at Stony Brook  
chris.jacobsen@stonybrook.edu

## INTRODUCTION

Soft x-ray microscopy uses X-rays with an energy of 100-1000 eV, or a wavelength of about 1-10 nm. The wavelength is much smaller than that of visible light, giving the potential for high spatial resolution imaging. The photon energy is well matched to inner-shell electron energies in low-Z elements. In particular, by operating between the *K* edges of carbon and oxygen, one has good intrinsic contrast between organic material and water and good penetration in micrometer-thick specimens (see figure below). Soft x-ray microscopy is therefore well suited to the study of specimens like single biological cells. For more info, see:

D. Sayre *et al.*, *Ultramicroscopy* 2, 337 (1977).

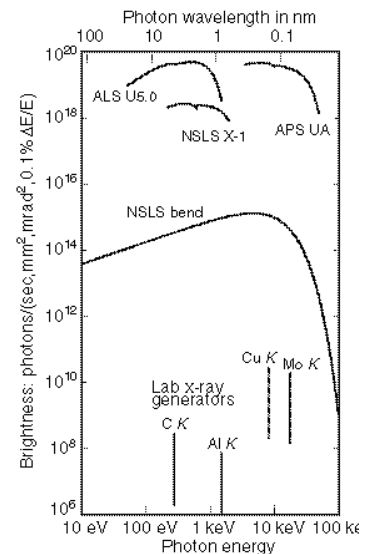
J. Kirz, C. Jacobsen, and M. Howells, *Q. Rev. Biophysics* 28, 33-130 (1995)

J. Thieme *et al.*, eds., *X-ray Microscopy and Spectromicroscopy* (Springer, Berlin, 1998)

## X-RAY MICROSCOPY AT STONY BROOK

The x-ray microscopy program at Stony Brook started in the 1970s as a collaboration between Janos Kirz and David Sayre of IBM, and led to the development of scanning transmission x-ray microscopes us-

ing zone plate optics. After experiments at SSRL at Stanford, a dedicated microscope beamline using synchrotron radiation was built with Malcolm Howells and Harvey Rarback at the NSLS in the early 1980s (U-15). By 1991, two microscopes had begun to operate at the X-1A undulator beamline and Chris Jacobsen had joined the Stony Brook faculty. The X-1A beamline now hosts two room temperature scanning transmission x-ray microscopes (STXMs), and a cryo STXM for studies of radiation-sensitive



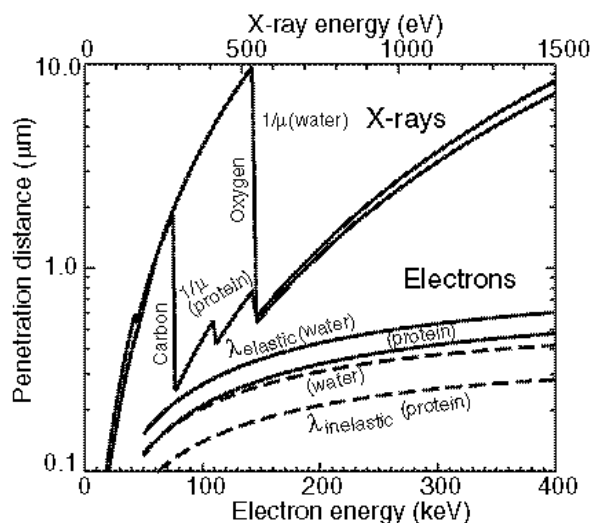
specimens. The program is funded by the National Science Foundation and by the National Institutes of Health. For more information, including a list of publications, see:

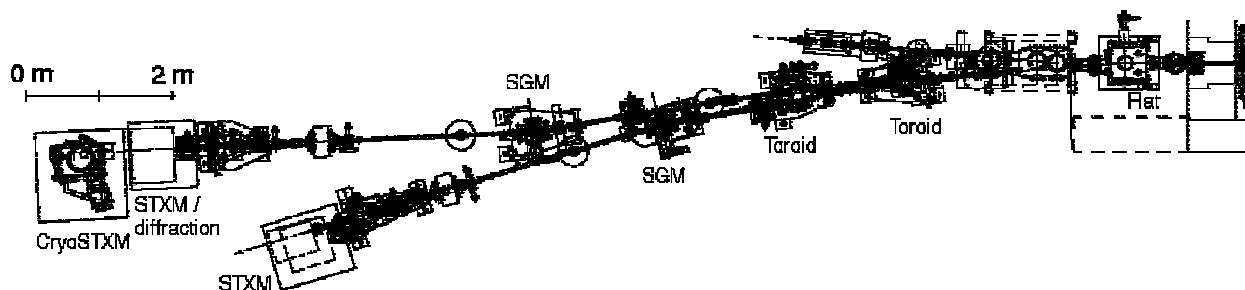
<http://xray1.physics.sunysb.edu>.

## THE X-1A UNDULATOR BEAMLINE

Undulators provide x-ray beams that are tunable in energy and well collimated. Their time-averaged brightness is about  $10^{10}$  times that of the laboratory sources available just a few decades ago. The X-1A undulator (with 37 periods of length  $\lambda_0=80$  mm) on the low-emittance X-ray Ring of the NSLS provides a bright soft x-ray beam with about 3 coherent modes in the vertical and 100 modes in the horizontal. STXM and other coherent illumination experiments are therefore able to share the beam with the X-1B spectroscopy beamline.

The X-1A beamline has two optically identical branches. In each case, a toroidal mirror is used for horizontal focusing onto the entrance slit of a horizon-



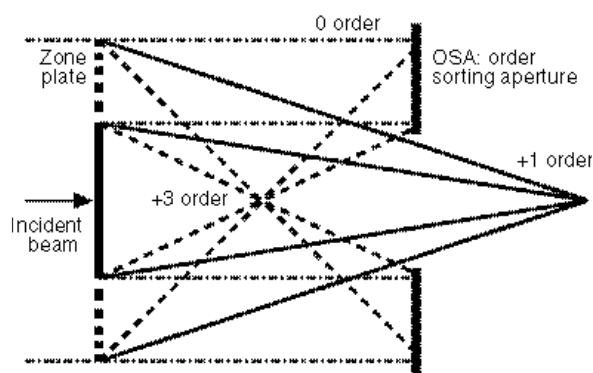


tally dispersing monochromator, and vertical focusing to the monochromator exit slit. The spherical grating monochromator (SGM) has an adjustable resolving power of 1000 to 5000, giving an energy resolution better than 0.1 eV for quantitative spectromicroscopy using X-ray Absorption Near-edge Structure (XANES) resonances.

As of mid-1999, each end station is home to a room temperature STXM. One end station is shared with a cryo STXM, while the other end station is shared with other coherent optics experiments such as diffraction and holography. A specimen preparation lab next to the beamline is equipped with optical microscopes, cell culture facilities, and other equipment. For more information on the beamline, see:

B. Winn *et al.*, *Proc. SPIE* 2856, 100 (1996)

are made by electron beam lithography, as originally proposed by David Sayre. The early Stony Brook microscopes used zone plates made in Dieter Kern's lab at IBM.



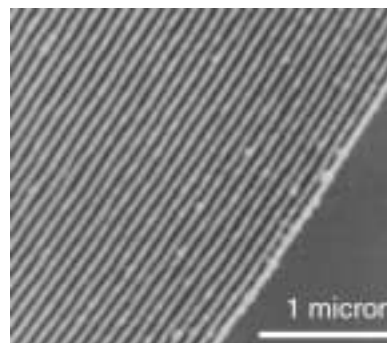
## FRESNEL ZONE PLATES FOR X-RAY MICROSCOPY

Because anything that refracts soft X-rays also strongly absorbs them, we use diffractive optics for high resolution focusing. Fresnel zone plates are circular diffraction gratings that have a spatial resolution limited to the width of the finest, outermost zones. In a STXM, they must be used with an order sorting aperture to isolate the first order focus.

Albert Baez first suggested the use of zone plates for x-ray microscopy, and the first x-ray zone plates to reach submicron resolution were made by G. Schmahl *et al.* in Göttingen, Germany. Today most zone plates

In a collaboration between Stony Brook and Don Tennant of Lucent Technologies Bell Laboratories, we fabricate Fresnel zone plates using a JEOL JBX-6000FS electron beam lithography machine. This machine (located at Bell Labs, Holmdel) is able to direct 1 nA of current into a 5-7 nm spot, with laser interferometer control of field precision. A trilevel resist process developed at Bell Labs is used to produce high aspect ratio structures such as is needed for high efficiency zone plates.

We have in use at X-1A zone plates with finest zone widths as small as 30 nm, and diameters as large as 160  $\mu\text{m}$ . Zone plates with finest zone widths as small as 18 nm have also been tested, and efforts are underway to make improved zone plates

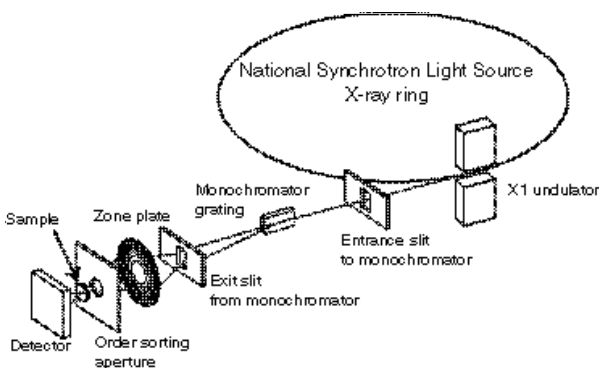


40 nm wide outermost zones in a 120 nm thick Ni zone plate

available for use. While zone plates are used for imaging in TXMs, they are used to produce a far-field focus in the STXM. In fact, we believe that our zone plates produce the finest far-field focus of electromagnetic radiation of any wavelength. For more information, see: S. Spector, C. Jacobsen, and D. Tennant, *J. Vac. Sci. Techn. B* 15, 2872–2876 (1997)

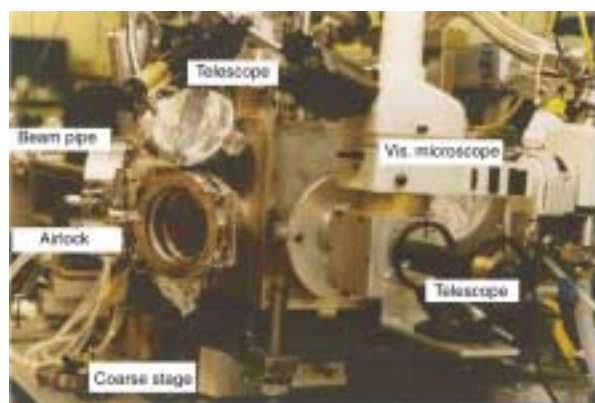
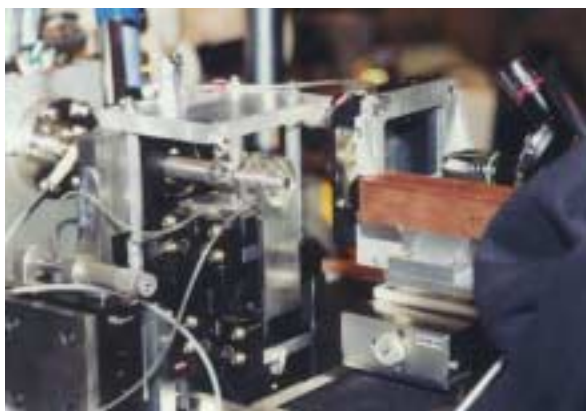
## SCANNING TRANSMISSION X-RAY MICROSCOPES

At Stony Brook, we have pioneered the development of scanning x-ray microscopes with Fresnel zone plate optics, beginning with a scanning transmission



x-ray microscope (STXM) at the NSLS in 1981. The optical configuration of STXMs (above) is well matched to the optics of high energy resolution grating monochromators. Radiation damage to the specimen is minimized because the Fresnel zone plate (with 10-20% efficiency) is positioned before rather than after the specimen. Scanning microscopes can image both large (millimeter) and small (micrometer) fields of view, and other signals besides transmission can be used (e.g., luminescence, photoemission).

At the X-1A beamline, we have two types of STXM. One microscope works with room temperature specimens in an atmospheric pressure air or helium environment, and can deliver images and absorption spec-



tra at the resolution limit of the zone plate optics used (presently about 35 nm). This microscope, which was newly redesigned in 1998 with support from the U.S. Department of Energy, is able to image either wet or dry specimens.

For radiation-sensitive specimens, we have developed a cryo STXM in which the sample is held at liquid nitrogen temperature. This allows us to image cells which are rapidly frozen from cell culture (i.e., a living state) with little or no limit due to radiation damage. The microscope has also been used for studies of other radiation sensitive specimens such as hydrated polymers, and with tensile holders in collaboration with Dow Chemical. For more information, see:

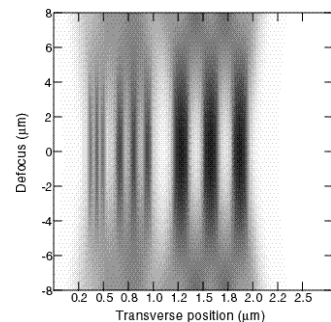
C. Jacobsen *et al.*, *Opt. Comm.* 86, 351–364 (1991)

J. Maser *et al.*, in J. Thieme *et al.*, eds., *X-ray Microscopy and Spectromicroscopy* (Springer-Verlag, Berlin, 1998).

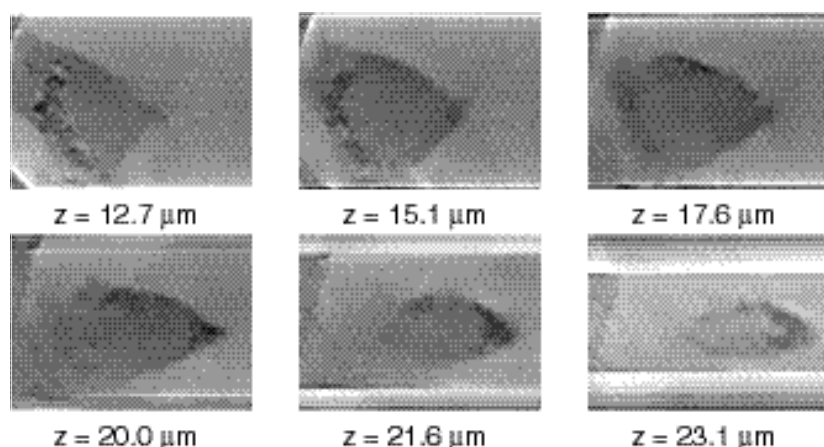
## EXAMPLES

### Tomography of frozen hydrated cells

Because zone plate lenses currently have relatively small numerical aperture (N.A.) of about 0.05, the X-Y or transverse resolution  $0.61\lambda/(N.A.)$  can be quite high while the depth of focus of about  $2\lambda/(N.A.)^2$  can be large. An example calculation is shown at right. The consequence of this is that samples several micrometers thick can be rotated through the depth of focus of the microscope, allowing one to obtain high-resolution pro-



Simulated images of 33, 71, and 148 nm wide bars, assuming a 45 nm outermost zone width at a wavelength of  $\lambda=2.4$  nm, showing a 8 μm depth of focus in this case.



**Slices through the reconstruction volume of a mouse 3T3 cell. These slices can be thought of as images of 100 nm thick slices at various depths through a block of ice containing the specimen. At each plane, different cell components can be visualized. Each image field is 32  $\mu\text{m}$  wide.**

jections through the sample at high resolution. This image sequence can then be processed using a variety of tomography reconstruction algorithms to deliver a three-dimensional representation of the sample.

Soft x-ray tomography of dried specimens was first demonstrated at X-1A by Haddad *et al.* [*Science* 266, 1213–1215 (1994)]. To do tomography with radiation-sensitive samples like biological cells, we had to wait for the development of the cryo STXM because the specimen must remain unchanged through the image sequence. We have then taken mouse 3T3 fibroblasts from cell culture, plunge-frozen them in liquid ethane, and acquired a tomographic data set in the cryo STXM. The image series was then processed using algebraic reconstruction tomography (ART) algorithms to yield the reconstruction shown below. For more information, see:

Y. Wang *et al.*, *J. Microscopy* 197, 80–93 (2000).

### **XANES spectroscopy of biomolecules**

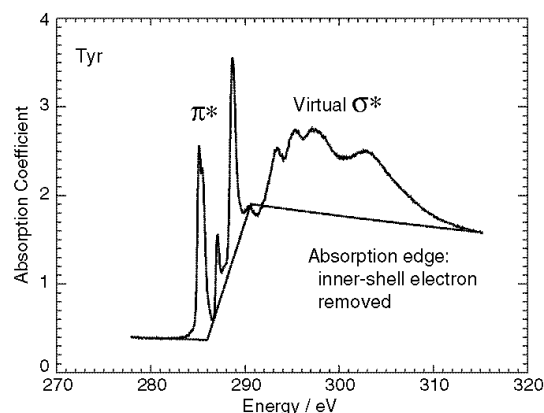
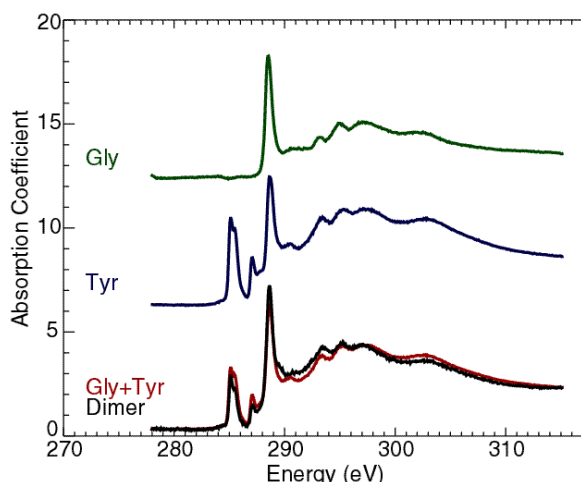
When the energy of an x-ray is increased to be at or above the binding energy of an inner-shell electron, the electron can be completely removed from the atom and the absorption cross section makes a step-like increase (shown at right). Near the edge, the electron can also be promoted to weakly bound states, such as those produced by molecular orbitals. These states give rise to X-ray Absorption Near-Edge Structure or XANES resonances, and these resonances depend on the chemical binding state of the atom.

At the carbon absorption edge, we have acquired absorption spectra of the 20 amino acids used as building blocks for proteins [Boese, Osanna *et al.*]. These absorption spectra can be used as a test for theoretical

calculations of the spectra based on molecular models [Carravetta *et al.*]. The presence of the peptide bond does not greatly alter the carbon edge XANES spectrum, so that the weighted sum of two monomer spectra closely approximates the measured spectrum of a dipeptide (see below). This raises the possibility of predicting the XANES spectra of proteins from knowledge of their amino acid content, and thereby using the intrinsic contrast differences of a sample to identify regions of locally high concentration of a protein within a cell. For further information:

J. Boese, A. Osanna, *et al.*, *J. Electr. Spectr. Rel. Phenom.* 85, 9–15 (1997)

V. Carravetta *et al.*, *J. Chem. Phys.* 109, 1456–1464 (1998)



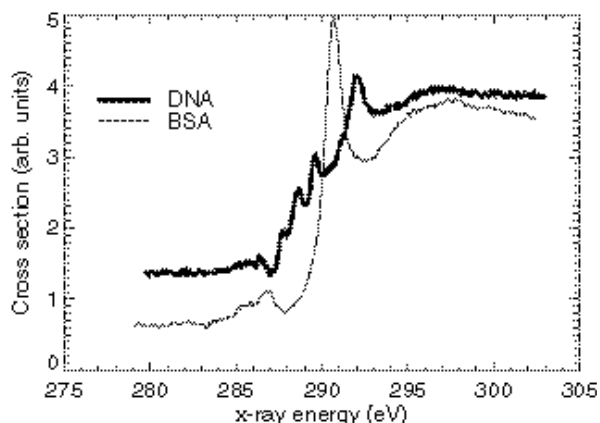
**Carbon XANES absorption spectrum of tyrosine, showing the step-like absorption edge and XANES resonances corresponding to different molecular orbitals [Boese, Osanna *et al.*].**



## Spectromicroscopy in biology

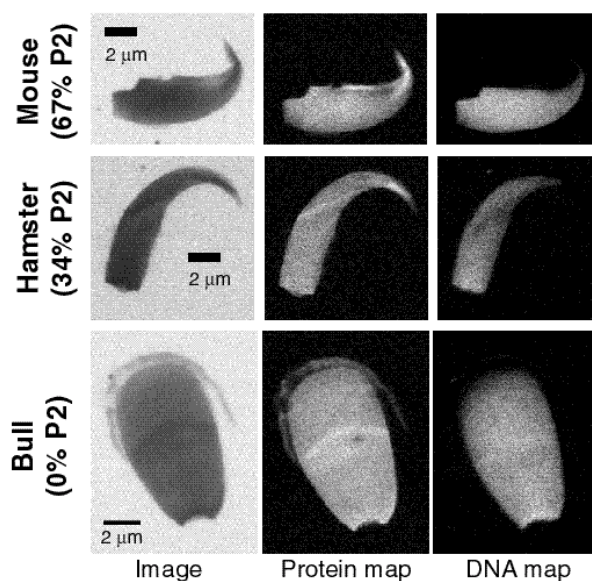
By taking images at photon energies at and away from an element's XANES resonances, images can be derived which highlight regions of high concentration of certain bonding states of the element by a technique called *spectromicroscopy* [see *e.g.*, Ade, Zhang *et al.*, *Science* 258, 972–975 (1992)].

This has been applied to understand the role of protamines in the packing of DNA in sperm [Zhang, Balhorn *et al.*]. Sperm from different species naturally have ratios of two proteins, protamine II to protamine I, that vary from 0% to 67% and more, whereas in other species (including humans) protamine II deficiencies are associated with infertility. It was therefore desired to measure the protein to DNA ratio to see whether protamine II replaces protamine I, or instead if it supplements protamine I in DNA packing. Because



a large fraction of sperm from a given sample can be defective, it is important to measure total protein to DNA content in individual sperm cells. The carbon XANES spectra of protein and DNA (shown above) were found to be sufficiently different that XANES spectromicroscopy could be used to measure the protein and DNA content of individual sperm. This was done by taking a series of six images of an air-dried sperm at energies varied around 290 eV, and processing the images to yield the desired maps (shown above, right). This process was carried out for species with different protamine II/protamine I ratios, with many sperm from each species analyzed. The conclusion of this study was that protamine II replaces protamine I, rather than somehow binding to the protamine I complex.

Dried specimens were used in this first study to ensure that the specimen remained unchanged by radiation damage while multiple images were acquired. Studies of this sort on frozen hydrated specimens, us-

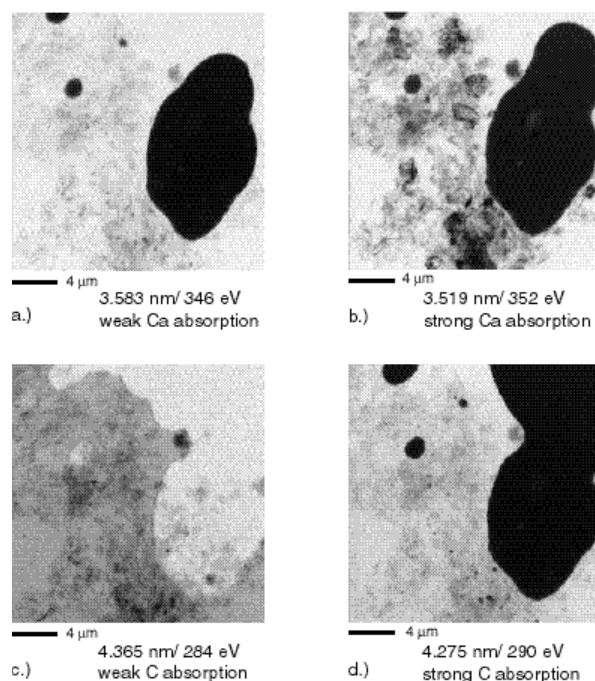


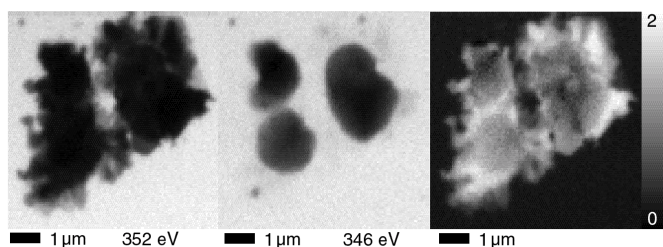
ing the cryo STXM described earlier, are now underway. For more information, see:

X. Zhang, R. Balhorn *et al.*, *J. Struct. Biol.* 116, 335–344 (1996)

## Spectromicroscopy of colloidal, environmental, and soil science specimens

Soft X-ray microscopes offer especially favorable contrast mechanisms for studying hydrated colloidal, environmental, and agricultural systems. Unlike in electron microscopy, samples can easily be examined in transmission in a hydrated state at atmospheric pressure without any pretreatment and with an approximately tenfold higher spatial resolution than achiev-



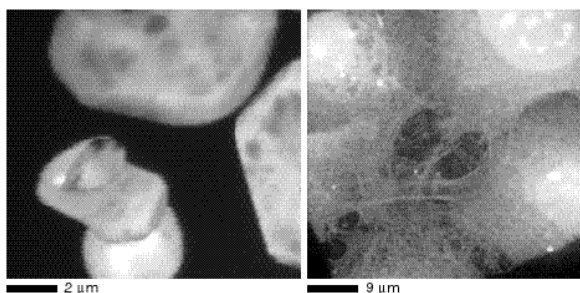


able in visible light microscopy.

Oil in water emulsions can be stabilized by many solid colloids, such as clay minerals. One new type of solid stabilized emulsion contains the same amount of montmorillonite (clay mineral; negatively charged) and Ca/Al layered double hydroxide (LDH; positively charged). X-ray microscopy allows one to better understand the structure of the heterocoagulates. Oil can be distinguished from water by taking images on either side of the carbon absorption edge, and calcium-rich double hydroxides can be distinguished from clay by taking images on and off a calcium absorption resonances (previous page). These studies with the X-1A STXM therefore make it possible to image at high resolution the separate components of the emulsion. Emulsions of this sort may be able to act as substitutes for classical emulsifiers, but with more benevolent environmental impact.

The image above shows an oil-in-water emulsion, containing only Ca/Al-LDH as an emulsifying agent. The colloids are located in the interface between oil and water and are not as spread out as in the clay/LDH emulsions. Quantitative mapping of calcium allows unambiguous identification of the oil droplets inside the Ca/Al-LDH envelope. For more information, see: S. Abend, N. Bonnke, U. Gutschner, and G. Lagaly, *Colloid Polymer Sci.* 276, 730 (1998)

U. Neuhausler, S. Abend, C. Jacobsen, and G. Lagaly, *Colloid Polymer Sci.*, 277, 719-26 (1999)

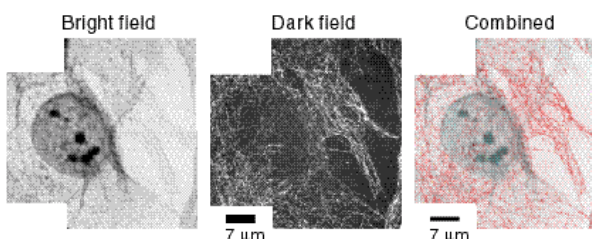


**Scanning luminescence x-ray microscope (SLXM) image of phosphor grains (left; see [1]) and Tb-labeled fibroblasts (right; see [2]).**

## Labeling of biological specimens

In biological microscopy, one is often interested in knowing not just about overall structure, but in knowing the location of sites of specific biochemical activities in a cell. This is beautifully done in visible light microscopy using fluorescent labels, and decades of research have yielded a powerful range of labels. In electron microscopy, immunogold labeling has also undergone considerable development for higher resolution imaging of epitope location. In x-ray microscopy, two labeling approaches have been developed at Stony Brook.

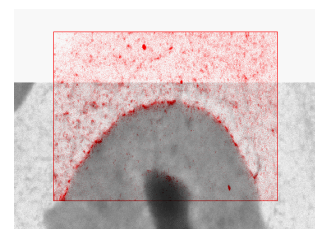
One approach involves the use of luminescent labels that emit visible light under x-ray irradiation [1]; because the scanned x-ray beam generates the signal, the image resolution is determined by the zone plate focus rather than by the resolution of the visible light



Bright field, dark field and combined (dark field in red) images of HF fibroblast labeled with 20 nm gold and silver enhanced to a mean particle size of 50 nm (labeling by K. Hedberg; see [3]).

collecting optics. This approach has been shown to make high resolution imaging possible [1], and efforts are underway at Lawrence Berkeley Laboratory to develop appropriate luminescent probes [2].

Another approach involves the use of antibody-conjugated gold labels. While gold labels can be seen in bright field images, it is especially advantageous to image them in dark field mode where one can easily see gold labels even in



Combined bright field/dark field image showing labeling of the nuclear lamina (from [4]).

heavily absorbing regions like cell nuclei [3,4]. This technique will become more promising as the resolution of x-ray microscopes improve, so that suitably small gold labels can be used. For further information, see: [1] C. Jacobsen *et al.*, *J. Microscopy* 172, 121-129 (1993)

[2] M. Moronne, *Ultramicroscopy* 77, 23-36 (1999)

[3] H. Chapman *et al.*, *Ultramicroscopy* 62, 191-213 (1996)

[4] S. Vogt, M.A. thesis, SUNY Stony Brook (1997).

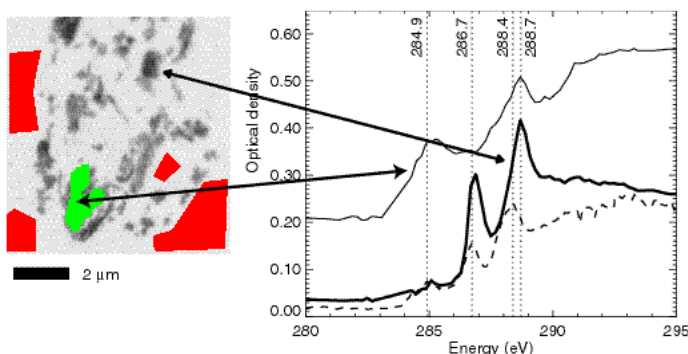
## Carbon in Interplanetary Dust

G. Flynn, SUNY Plattsburgh; L. Keller, MVA Associates; S. Wirick and C. Jacobsen, SUNY Stony Brook

The Earth experiences a continuous, planet-wide rain of interplanetary dust, with about 40,000 tons of particles from 5 to 500 microns in size accreting annually. Samples of the smallest interplanetary dust particles (IDPs), from 5 to 25 microns in size, are collected from the Earth's stratosphere by NASA research aircraft. Some of these IDPs are the most primitive samples available for laboratory analysis of the dust from which our Solar System formed. A few IDPs are so primitive that they have non-Solar deuterium/hydrogen isotopic ratios, indicating they never fully equilibrated into the Solar System mix. The organic content of IDPs is particularly important because modeling suggests IDPs may have delivered to the surface of the early Earth the pre-biotic organic compounds required for the origin of life.

All but one of the twelve IDPs examined using the STXM have C-XANES spectra indicating the presence of significant quantities of organic carbon, demonstrating that organic carbon is far more abundant in the IDPs than previously suspected. Assuming ~2 wt-% organic content, the accretion of interplanetary dust contributes more than  $10^4$  kg/yr of unpyrolyzed (not heated above 600° C) organic matter to the Earth.

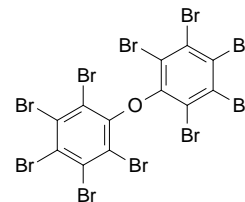
One of these IDPs, L2009\*E2, is particularly interesting. L2009\*E2 is dominated by micron and submicron-sized olivine and pyroxene grains, submicron spheroids of glass [which Bradley (*Science* 265, 925-929, 1994) suggests may be surviving interstellar grains], and carbonaceous material. Spots in this IDP have deuterium excesses of 400 per mil, well above that found in Solar System matter, indicating L2009\*E2 is an extremely primitive IDP. STXM analysis identified numerous carbon-rich regions, some as small as ~1/4 micron in size. Unlike the other more equilibrated IDPs examined, which show only a single type of organic carbon C-XANES spectrum, L2009\*E2 has several distinct spectra, and appears to contain at least three different organic carbon species separated by distances of only microns. This is consistent with the low degree of equilibration of L2009\*E2. Comprehensive C-XANES spectroscopic analysis of the most primitive IDPs, like L2009\*E2, offers the opportunity to determine the types and relative abundances of the carbonaceous matter present in the early stages of Solar System formation, and may also allow identification and analysis of pre-solar organic matter.



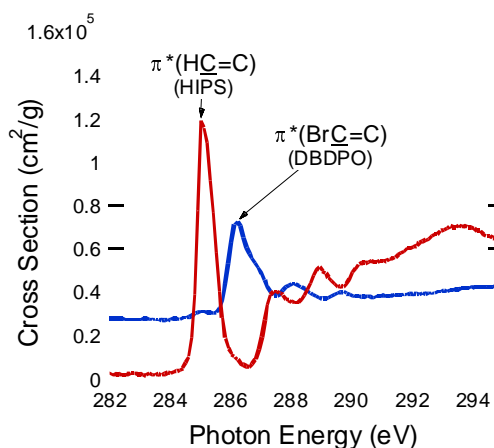
## NEXAFS Microanalysis of Polymers using STXM

G.E. Mitchell and E. G. Rightor, Dow Chemical, and collaborators

Modern polymeric materials often contain many different types of additives, fillers or modifiers to alter the physical or chemical properties of the polymer. These additives are sometimes partially miscible with one or another phase of the polymer and the properties imparted by the additive are dependent on the phase in which the additive resides. As one example, we are using STXM to determine the location of flame retardants in rubber modified high impact polystyrene. Poly-brominated flame retardants are added to high impact polystyrene (HIPS) to improve the ignition resistance as these additives act as free radical traps in the vapor phase during burning. The structural formula for one flame retardant additive, decabromodiphenyl oxide (DBDPO) is presented at right.

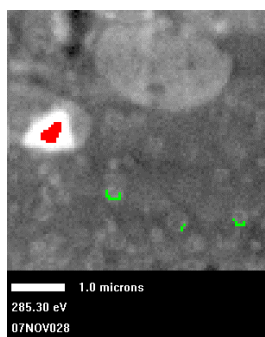


The NEXAFS spectra of DBDPO and the various HIPS phases are substantially different from each other, and

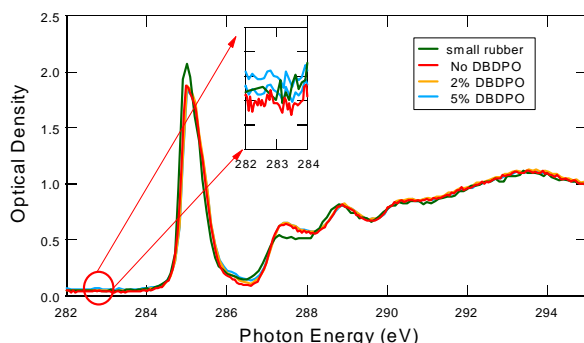


A comparison of the NEXAFS spectra of the rubber phase from HIPS and DBDPO.





STXM image of the sample with DBDPO from an image stack with photon energy of 285.3 eV. The pixels in green indicate those from which the spectrum was extracted and the red pixels indicate the source for the incident intensity data.



this provides a useful handle to determine the dissolved flame retardant in the various HIPS microphases. Two obvious differences in the spectra of the polymer and flame retardant are: (1) the intensity of the signal below the C(1s) edge is much higher for the flame retardant; (2) the energy of the most intense resonant feature in the spectrum is 285.1 eV ( $C(1s) \rightarrow \pi^*(C=C)$ ) for HIPS and 286.6 eV for DBDPO ( $C(1s) \rightarrow \pi^*(C=C)$  for the C atoms bonded to the Br atoms). The spectra are compared only for the rubber phase (previous page), but the observations (1-2) are true for all the phases.

To determine the dissolved or finely dispersed flame retardant, image stacks of the polymer with DBDPO were acquired and spectra were derived from each phase. These spectra were then compared to calculated spectra made by summing together spectra of the various phases in a HIPS sample (with no flame retardant) with the spectrum of the flame retardant. The figure above presents an example from the analysis of the DBDPO / HIPS. In the image the lighter colored phases are rubber phases that enhance the impact resistance of this material. This polymer has two different size particles of the (polybutadiene) rubber phase ( $\sim 2$  and  $<1 \mu m$ ) that are clearly visible in the image. Three different calculated spectra are compared (0, 2 and 5% DBDPO). These results indicated that the rubber phase contained about 2% flame retardant by weight.

## Studies of Organic Geochemistry and Fuel Chemistry

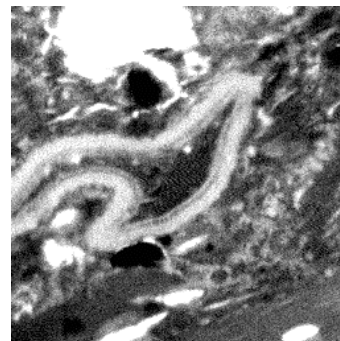
*George Cody, Carnegie Institute, and collaborators*

Fundamental studies of the chemistry of complex solids in the fields of organic geochemistry and fuels chemistry have benefited enormously over the past decades from developments in instrumental analytical

condensed macromolecular systems. These are very powerful techniques, yet they suffer from an unavoidable limitation: chemical information is obtained via integration across the bulk chemistry of a given sample. In most cases of interest to either scientific field, it has been long recognized that significant microscopic and nanoscale sample heterogeneity exists; in many cases, the crucial chemistry occurs within discrete regions. Dilution of the signal of such chemistry unavoidably results with analytical integration over microscopic heterogeneities. In systems where parallel chemistries evolve in different submicroscopic domains, deconvolution of discrete chemical evolution pathways may become impossible. Such mixing of signals can lead to severe misunderstanding of chemical processes within heterogeneous carbonaceous solids.

Recent developments in soft X-ray optics and instrumental design at the X1A beam line now make it possible to obtain organic functional group chemistry down to 50 nm length scales. This state of the art instrumentation now opens up the possibility to probe chemistry within discrete domains within complex carbonaceous solids and unravel the chemistry associated with natural and industrial processes. As part of an on-

methods. In particular  $^{13}C$  solid state nuclear magnetic resonance spectroscopy and pyrolysis gas chromatography coupled with gas chromatography/mass spectrometry now allow us to interrogate organic solids for quantitative molecular and functional group concentrations; thus one can now follow and characterize organic chemistry within



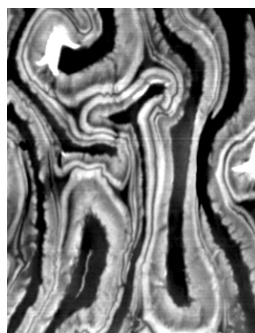
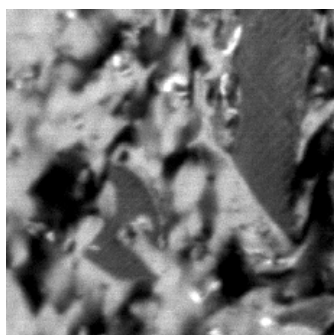
C-XANES image at 285 eV of ca. 70 Ma sporopollenin in Upper Cretaceous Coal. The resistant spore exine membrane is ca. 2  $\mu m$  thick. A C-XANES study of microspores across a range of organic rich rocks reveals systematic evolution in the chemistry within the preserved cell membrane with thermal metamorphism (Cody et. al. 1996).



going project in exploring the use of this new analytical method in the areas of organic geochemistry the application of soft x-ray spectral microscopy has been investigated. These include the geochemical evolution of biomacromolecular ensembles (e.g., cell membranes with pressure, temperature, and time); studies of the biodegradation of chemically resistant biopolymers under aerobic and anaerobic conditions; the study of changes in the microscopic constituents of coal across rank/thermal maturation series; and the study of sub-microscopic nematic phase transitions in carbonaceous solids with thermal treatments relevant to the formation and structural development of metallurgical cokes used for smelting and refining. Each of these study areas shares the same intrinsic complexity; the important chemical transformations occur within discrete regions generally less than a 1  $\mu\text{m}$  across. Examples of specific applications are given.

Imaging chemical differentiation within the membrane of Eocene (45 Ma) Tracheid cells. C-XANES microanalysis of the structurally distinct regions across the cell wall allows for a clear assessment of the geochemical evolution of structural biopolymers. STXM analysis will allow for the in-situ analysis of intramembrane chemistry within the preserved remains of a broad range of ancient organisms adding a powerful tool for paleobotanical research directed at unraveling the evolution and diversification of plants in the middle and possibly early Paleozoic era.

Nematic Texture in thermal petroleum coke revealed with highly polarized x-rays tuned to 285 eV. Dark regions correspond to molecular orientation such

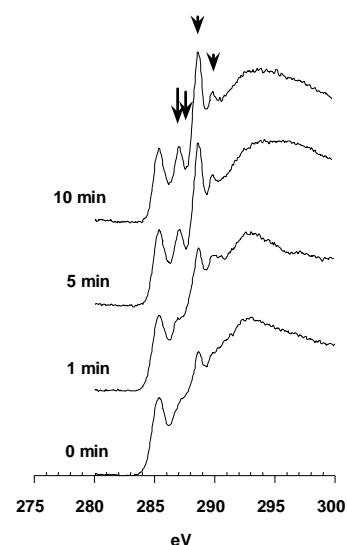


that  $\pi^*$  orbitals are perpendicular to the electric vector of the polarized x-ray beam. Studies of experimental cokes using soft x-ray linear dichroism studies on carbon's 1s absorption edge is being used to resolve the physical chemistry of

these complex systems.

C-XANES spectral microscopy requires extremely

thin samples. This requirement has been exploited to probe the photochemical oxidation of coal surfaces. Under ambient oxygen conditions with blue light irradiation significant alteration of the chemistry of coal occurs within minutes. Significant differences in the spectroscopic response to these experiments are observed across a suite



of coals of different rank. These results provide quantitative support for a new series of less sensitive techniques being developed to assess thermal maturity for oil exploration. In general, an assessment of photochemical oxidation is important for the weathering and recycling of organic matter related to earth's global carbon cycle. For more information, see:

Cody, G. D., Ade, H., Wirick, S., Mitchell, G. D., and Davis, A., *Organic Geochemistry* 28 (1998), 441-456.

Cody, G. D., Botto, R. E., Ade, H., Wirick, S., *International Journal of Coal Geology* 32 (1996), 69-86.

Cody, G. D., Ade, H., Behal, S., Botto, R. E., Disko, M., Kirz, J., Wirick, S., *Energy & Fuels* 9 (1995), 525-533.

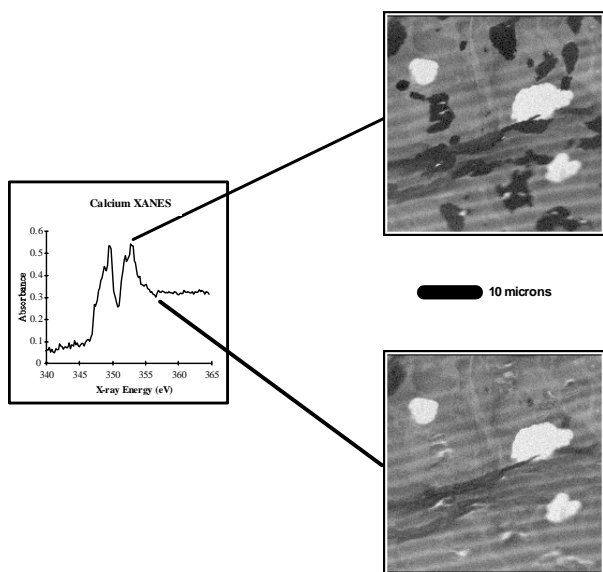
Cody, G. D., Ade, H., Behal, S., Botto, R. E., Disko, M., Kirz, J., Wirick, S. C., *Energy & Fuels* 9 (1995), 75-83.

### Calcification of Bioprosthetic Heart Valves

Carl Zimba (NIST) and Naomi Eidelman (ADAHF)

Calcification of bioprosthetic heart valves (BHV) is the major cause of their failure with time. The causes of the calcification are not fully understood. Previous attempts of characterizing and mapping calcified BHV's required tissue processing methods that could alter the inorganic and organic constituents of the calcified deposits and could not give direct information about their chemical composition.

The images and Calcium NEXAFS spectrum shown below were obtained from a 100 nm thick cross-section of an explant sample using the scanning transmission x-ray microscope (STXM) at Beamline X1A. The sample was a 1  $\text{cm}^2$  piece of bovine pericardium which was pretreated with gluteraldehyde, implanted subdermally in a laboratory rat for 28 days, retrieved, washed with distilled water and lyophilized to remove



excess water. A small piece of the sample was mounted in epoxy and then cryo-microtomed at -60 C. Other analyses on macroscopic samples have indicated that there is 12.7% Ca in the form of biological apatite and that there is 18.3%  $\text{PO}_4$  per dry tissue.

The NEXAFS spectrum below is typical of inorganic calcium, exhibiting two distinct absorption bands at x-ray energies near 349.5 and 353.0 eV. The image corresponding to absorption maxima in the Ca NEXAFS spectrum clearly shows dark areas of 1 to 8 microns in size that correspond to areas of Ca mineralization. In contrast, the other image taken at an energy above the absorptions, show no such features and indicate the density and thickness variations within the cross-section. In each of the images, the white areas correspond to voids in the sample while the horizontal lines of darker and lighter intensity are due to variation in sample thickness caused during sectioning.

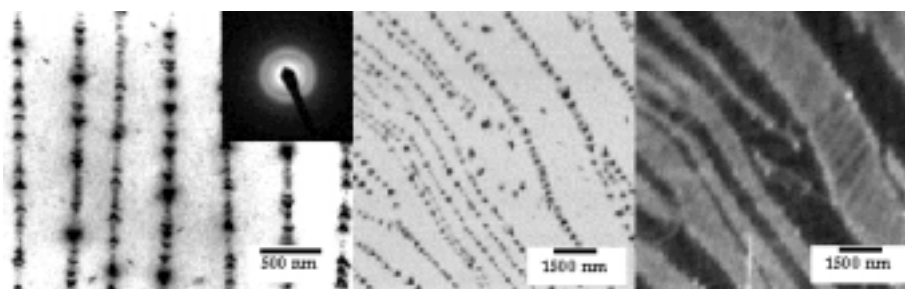
### Orientation is Self-Assembled Diblock Copolymers

*Carl G. Zimba (NIST), Edwin L. Thomas (MIT), Christopher Ober (Cornell)*

Block copolymers have been extensively investigated using a wide variety of analytical techniques, including electron microscopy, x-ray scattering, and optical microscopy. These techniques have yielded considerable information about the morphology and organization of these novel materials. NEXAFS microscopy is a complementary tool that

can provide unique information. We have investigated the novel molecular organization of a high molecular weight block copolymer having a polystyrene (PS) coil block of 9K molecular weight and a main-chain poly(hexyl isocyanate) (PHIC) rigid rod block of 245K molecular weight. This class of block copolymers form new molecular architectures and morphologies due to the competition between the microphase separation of the PS and PHIC blocks into periodic structures and the tendency of the PHIC block to form anisotropically ordered structures.

A typical TEM image obtained is shown below, clearly showing a microphase separated morphology with long-range order over tens of microns. The PS domains, stained with  $\text{RuO}_4$ , appear as dark regions shaped somewhat like arrowheads, alternating in direction between adjacent PS-rich domains, while the PHIC regions appear as largely featureless light regions between rows of PS domains. The SAED pattern (inset of figure), obtained from a sample area of 20 lamellae, shows a superposition of two distinct single crystal-like PHIC patterns that indicate that the PHIC chain axis alternates between  $+45^\circ$  and  $-45^\circ$  with respect to the geometric normal of the lamellae layers. Using an x-ray energy of 285.0 eV, corresponding to the phenyl carbon resonance of the PS, the NEXAFS image clearly shows a similar arrowhead morphology as the TEM image, albeit at lower spatial resolution. Changing the x-ray energy to 288.5 eV, corresponding to the carbonyl resonance of the PHIC, images detailing the structure of the PHIC layers can be obtained, information that is not available with TEM. In this image, the PHIC domains appear as layers of alternating intensity separated by the PS domains that appear as white pearls. The intensity variation of the PHIC layers arises from dichroic absorption of the polarized synchrotron radiation by the oriented carbonyl moiety of the PHIC. In contrast to the SAED pattern, the NEXAFS image is able to give detailed information about the orientation of individual PHIC domains. In fact, there is also much fine structure within the PHIC domains that is present, although not presently understood.



## REPRESENTATIVE PUBLICATIONS

- S. Vogt, H. N. Chapman, C. Jacobsen, and R. Medenwaldt, "Dark field x-ray microscopy: the effects of condenser/detector aperture," *Ultramicroscopy*, vol. 87, pp. 25-44, 2001.
- H. Ade and S. G. Urquhart, "NEXAFS spectroscopy and microscopy of natural and synthetic polymers," in *Chemical Applications of Synchrotron Radiation* (T. K. Sham, ed.), Singapore: World Scientific Publishing, 2001.
- A. P. Hitchcock, I. Koprinarov, T. Tyliczszak, E. Rightor, G. E. Mitchell, M. T. Dineen, F. Hayes, W. Lidy, R. D. Priester, S. G. Urquhart, A. P. Smith, and H. Ade, "Optimization of scanning transmission x-ray microscopy for the identification and quantitation of reinforcing particles in polyurethanes," *Ultramicroscopy*, vol. 88, pp. 33-49, 2001.
- A. P. Smith, H. Ade, S. D. Smith, C. C. Koch, and R. J. Spontak, "Anomalous phase inversion in polymer blends prepared by cryogenic mechanical alloying," *Macromolecules*, vol. 34, pp. 1536-1538, 2001.
- A. P. Smith, H. Ade, C. C. Koch, and R. J. Spontak, "Cryogenic mechanical alloying as an alternative strategy for the recycling of tires," *Polymer*, vol. 42, pp. 4453-4457, 2001.
- M. Feser, T. Beetz, M. Carlucci-Dayton, and C. Jacobsen, "Instrumentation advances and detector development with the Stony Brook scanning transmission x-ray microscope," in Meyer-Ilse et al. [185], pp. 367-372.
- C. Jacobsen, S. Abend, T. Beetz, M. Carlucci-Dayton, M. Feser, K. Kaznacheyev, J. Kirz, J. Maser, U. Neuhäusler, A. Osanna, A. Stein, C. Vaa, Y. Wang, B. Winn, and S. Wirick, "Recent developments in scanning microscopy at Stony Brook," in Meyer-Ilse et al. [185], pp. 12-18.
- C. Jacobsen, G. Flynn, S. Wirick, and C. Zimba, "Soft x-ray spectroscopy from image sequences with sub-100 nm spatial resolution," *Journal of Microscopy*, vol. 197, no. 2, pp. 173-184, 2000.
- A. R. Kalukin, B. Winn, Y. Wang, C. Jacobsen, Z. H. Levine, and J. Fu, "Calibration of high-resolution x-ray tomography with atomic force microscopy," *Journal of Research of the National Institute of Standards and Technology*, vol. 105, no. 6, pp. 867-874, 2000.
- J. Maser, A. Osanna, Y. Wang, C. Jacobsen, J. Kirz, S. Spector, B. Winn, and D. Tennant, "Soft x-ray microscopy with a cryo STXM: I. Instrumentation, imaging, and spectroscopy," *Journal of Microscopy*, vol. 197, no. 1, pp. 68-79, 2000.
- U. Neuhäusler, C. Jacobsen, D. Schulze, D. Stott, and S. Abend, "A specimen chamber for soft x-ray spectromicroscopy on aqueous and liquid samples," *Journal of Synchrotron Radiation*, vol. 7, pp. 110-112, 2000.
- U. Neuhäusler, S. Abend, S. Ziesmer, D. Schulze, D. Stott, K. Jones, H. Feng, C. Jacobsen, and G. Lagaly, "Soft x-ray spectromicroscopy on hydrated colloidal and environmental science samples," in Meyer-Ilse et al. [185], pp. 323-328.
- A. Osanna and C. Jacobsen, "Principle component analysis for soft x-ray spectromicroscopy," in Meyer-Ilse et al. [185], pp. 350-357.
- D. Tennant, S. Spector, A. Stein, and C. Jacobsen, "Electron beam lithography of Fresnel zone plates using a rectilinear machine and trilayer resists," in Meyer-Ilse et al. [185], pp. 601-606.
- Y. Wang, C. Jacobsen, J. Maser, and A. Osanna, "Soft x-ray microscopy with a cryo STXM: II. Tomography," *Journal of Microscopy*, vol. 197, no. 1, pp. 80-93, 2000.
- B. Winn, H. Ade, C. Buckley, M. Feser, M. Howells, S. Hulbert, C. Jacobsen, K. Kaznacheyev, J. Kirz, A. Osanna, J. Maser, I. McNulty, J. Miao, T. Oversluizen, S. Spector, B. Sullivan, S. Wang, S. Wirick, and H. Zhang, "Illumination for coherent soft x-ray applications: the new X1A beamline at the NSLS," *Journal of Synchrotron Radiation*, vol. 7, pp. 395-404, 2000.
- F. Polack, D. Joyeux, M. Feser, D. Phalippou, M. Carlucci-Dayton, K. Kaznacheyev, and C. Jacobsen, "Demonstration of phase contrast in scanning transmission x-ray microscopy: comparison of images obtained at NSLS X1-A with numerical simulations," in Meyer-Ilse et al. [185], pp. 573-580.
- C. Schmidt, J. Thieme, U. Neuhäusler, U. Schulte-Ebbert, G. Abbt-Braun, C. Specht, and C. Jacobsen, "Association of particles and structures in the presence of organic matter," in Meyer-Ilse et al. [185], pp. 313-318.
- A. P. Smith, H. Ade, C. C. Koch, S. D. Smith, and R. J. Spontak, "Addition of a block copolymer to polymer blends produced by cryogenic mechanical alloying," *Macromolecules*, vol. 33, pp. 1163-1172, 2000.
- A. P. Smith, H. Ade, C. M. Balik, C. C. Koch, S. D. Smith, and R. J. Spontak, "Cryogenic mechanical alloying of poly(methyl methacrylate) with polyisoprene and poly(ethylene-alt-propylene)," *Macromolecules*, vol. 33, no. 7, pp. 2595-2604, 2000.
- A. P. Smith, R. Spontak, C. Balik, C. Koch, S. Smith, and H. Ade, "High-energy mechanical alloying of poly(methyl methacrylate) with polyisoprene or poly(ethylene-alt-propylene) at cryogenic temperatures," *Macromolecular Materials and Engineering*, vol. 274, no. 1, pp. 1-12, 2000.
- A. P. Smith, J. S. Shay, R. Spontak, C. Balik, H. Ade, S. Smith, and C. Koch, "High-energy mechanical milling of poly(methyl methacrylate), polyisoprene and poly(ethylene-alt-propylene)," *Polymer*, vol. 41, no. 16, pp. 6271-6283, 2000.
- D. Slep, J. Asselta, M. H. Rafailovich, J. Sokolov, D. A. Winesett, A. P. Smith, H. Ade, and S. Anders, "The effect of an interactive surface on the equilibrium contact angle in bilayer poly-

- mer films," *Langmuir*, vol. 16, no. 5, pp. 2369-2375, 2000.
- D. A. Winesett, H. Ade, J. Sokolov, M. Rafailovich, and S. Zhu, "Substrate dependence of morphology in thin film polymer blends," *Polymer International*, vol. 49, no. 5, pp. 458-462, 2000.
- D. A. Winesett, S. Zhu, J. Sokolov, M. Rafailovich, and H. Ade, "Time-temperature superposition of phase separating polymer blend films," *High Performance Polymers*, vol. 12, pp. 599-602, 2000.
- H. N. Chapman, S. Vogt, C. Jacobsen, J. Kirz, J. Miao, Y. Wang, B. Winn, and T. Oversluizen, "A shutter-photodiode combination for UV and soft x-ray beamlines," *Journal of Synchrotron Radiation*, vol. 6, p. 50, 1999.
- C. Jacobsen and U. Neuhausler, "Soft x-ray optics and spectromicroscopy: potential for soil science specimens," in *Synchrotron Methods in Clay Science*, vol. 8, (Boulder, CO), pp. 183-206, Clay Minerals Society Workshop Lecture Series, 1999.
- C. Jacobsen, "Soft x-ray microscopy," *Trends in Cell Biology*, vol. 9, pp. 44-47, Feb. 1999.
- J. Miao, P. Charalambous, J. Kirz, and D. Sayre, "An extension of the methods of x-ray crystallography to allow imaging of micron-size non-crystalline specimens," *Nature*, vol. 400, pp. 342-344, 1999.
- U. Neuhausler, S. Abend, G. Lagaly, and C. Jacobsen, "Soft x-ray spectromicroscopy on solid stabilized emulsions," *Colloid and Polymer Science*, vol. 277, pp. 719-726, 1999.
- H. Ade, D. A. Winesett, A. P. Smith, S. Qu, S. Ge, S. Rafailovich, and J. Sokolov, "Phase segregation in polymer thin films: elucidations by x-ray and scanning force microscopy," *Europhysics Letters*, vol. 45, pp. 526-532, 1999.
- R. Giebler, B. Schulz, J. Reiche, L. Brehmer, M. Wühn, C. Wöll, A. Smith, S. Urquhart, H. Ade, and W. Unger, "NEXAFS-spectroscopy on ordered films of amphiphilic derivatives of 2,5-diphenyl-1,3,4-oxadiazoles," *Langmuir*, vol. 15, pp. 1291-1298, 1999.
- M. M. Moronne, "Development of x-ray excitable luminescent probes for scanning x-ray microscopy," *Ultramicroscopy*, vol. 77, pp. 23-36, 1999.
- A. P. Smith, R. Spontak, H. Ade, S. Smith, and C. Koch, "High-energy cryogenic blending and compatibilization of immiscible polymers," *Advanced Materials*, vol. 11, pp. 1277-1281, 1999.
- S. Urquhart, A. Hitchcock, A. Smith, H. Ade, B. Lessard, W. Lidy, E. Rightor, and G. Mitchell, "NEXAFS spectromicroscopy of polymers: overview and quantitative analysis of polyurethane polymers," *Journal of Electron Spectroscopy and Related Phenomena*, vol. 100, pp. 119-135, 1999.
- S. Urquhart, A. Smith, H. Ade, A. Hitchcock, E. Rightor, and W. Lidy, "Near-edge x-ray absorption fine structure spectroscopy of MDI and TDI polyurethane polymers," *Journal of Physical Chemistry*, vol. B 103, pp. 4603-4610, 1999.
- S. Zhu, Y. Liu, M. H. Rafailovich, J. Sokolov, D. Gersappe, A. Winesett, and H. Ade, "Confinement-induced miscibility in polymer blends," *Nature*, vol. 400, pp. 49-51, 1999.
- J. Boese, A. Osanna, C. Jacobsen, J. Kirz, E. Tall, and X. Zhang, "X-ray absorption near-edge structure of amino acids and peptides," in Thieme et al. [186], pp. III-89-93.
- M. Feser, M. Carlucci-Dayton, C. J. Jacobsen, J. Kirz, U. Neuhausler, G. Smith, and B. Yu, "Applications and instrumentation advances with the stony brook scanning transmission x-ray microscope," in *X-ray microfocusing: applications and techniques* (I. McNulty, ed.), vol. 3449, (Bellingham, Washington), pp. 19-29, Society of Photo-Optical Instrumentation Engineers (SPIE), 1998.
- C. Jacobsen and J. Kirz, "X-ray microscopy with synchrotron radiation," *Nature Structural Biology*, vol. 5 (supplement), pp. 650-653, 1998.
- C. Jacobsen, R. Medenwaldt, and S. Williams, "A perspective on biological x-ray and electron microscopy," in Thieme et al. [186], pp. II-93-102.
- J. Maser, C. Jacobsen, J. Kirz, A. Osanna, S. Spector, S. Wang, and J. Warnking, "Development of a cryo scanning x-ray microscope at the NSLS," in Thieme et al. [186], pp. I-35-44.
- J. Miao, D. Sayre, and H. N. Chapman, "Phase retrieval from the magnitude of the Fourier transforms of non-periodic objects," *Journal of the Optical Society of America*, vol. A 15, no. 6, pp. 1662-1669, 1998.
- D. Sayre, H. N. Chapman, and J. Miao, "On the extendibility of x-ray crystallography to noncrystals," *Acta Crystallographica*, vol. A 54, pp. 232-239, 1998.
- S. J. Spector, C. J. Jacobsen, and D. M. Tennant, "Zone plates for a scanning transmission x-ray microscope," in Thieme et al. [186], pp. IV-13-19.
- Y. Wang and C. Jacobsen, "A numerical study of resolution and contrast in soft x-ray contact microscopy," *Journal of Microscopy*, vol. 191, no. 2, pp. 159-169, 1998.
- H. Ade, D. A. Winesett, A. P. Smith, S. Anders, T. Stämmler, C. Heske, D. Slep, M. H. Rafailovich, J. Sokolov, and J. Stöhr, "Bulk and surface characterization of a dewetting thin film polymer bilayer," *Applied Physics Letters*, vol. 73, pp. 3775-3777, 1998.
- H. Ade, "NEXAFS and x-ray linear dichroism microscopy and applications to polymer science," in Thieme et al. [186], pp. III-3-14.
- H. Ade, "X-ray spectromicroscopy," in *Experimental Methods in the Physical Sciences* (R. Celotta and T. Lucatorto, eds.),



vol. 32, ch. 11, pp. 225-262, New York: Academic Press, 1998.

C. Buckley, N. Khaleque, S. J. Bellamy, M. Robbins, and X. Zhang, "Mapping the organic and inorganic components of bone," in Thieme et al. [186], pp. II-47-55.

R. Balhorn, R. E. Braun, B. Breed, J. T. Brown, D. Evenson, J. M. Heck, J. Kirz, I. McNulty, W. Meyer-Ilse, and X. Zhang, "Applications of x-ray microscopy to the analysis of sperm chromatin," in Thieme et al. [186], pp. II-29-46.

G. Cody, H. Ade, S. Wirick, G. Mitchell, and A. Davis, "Determination of chemical-structural changes in vitrinite accompanying luminescence alteration using C-NEXAFS analysis," *Organic Geochemistry*, vol. 28, pp. 441-456, 1998.

G. J. Flynn, L. P. Keller, C. Jacobsen, and S. Wirick, "Carbon mapping and carbon bonding state measurements on interplanetary dust particles," in *Lunar and Planetary Science*, vol. XXIX, (Houston, TX, USA), Lunar and Planetary Institute, 1998. Abstract 1159.

G. J. Flynn, L. P. Keller, C. Jacobsen, and S. Wirick, "Carbon and potassium mapping and carbon bonding state measurements on interplanetary dust," *Meteoritics and Planetary Science*, vol. 33 (supplement), no. 4, pp. A50-51, 1998.

G. J. Flynn, L. P. Keller, M. A. Miller, C. Jacobsen, and S. Wirick, "Organic compounds associated with carbonate globules and rims in the ALH84001 meteorite," in *Lunar and Planetary Science*, vol. XXIX, (Houston, TX, USA), Lunar and Planetary Institute, 1998. Abstract 1156.

G. J. Flynn, L. P. Keller, C. Jacobsen, and S. Wirick, "Carbon in Allan Hills 84001 carbonate and rim," *Meteoritics and Planetary Science*, vol. 33 (supplement), no. 4, p. A50, 1998.

S. Lindaas, B. Calef, K. Downing, M. Howells, C. Magowan, D. Pinkas, and C. Jacobsen, "X-ray holography of fast-frozen hydrated biological samples," in Thieme et al. [186], pp. II-75-86.

F. Polack, D. Joyeux, and D. Phalippou, "Phase contrast experiments on the NSLS-X1A scanning microscope," in Thieme et al. [186], pp. I-105-109.

D. Slep, J. Asselta, M. Rafailovich, J. Sokolov, D. Winesett, A. Smith, H. Ade, Y. Strzhemechny, S. Schwarz, and B. Sauer, "The phase separation of polystyrene and bromo-polystyrene mixtures in equilibrium structures in thin films," *Langmuir*, vol. 14, pp. 4860-4864, 1998.

A. P. Smith, C. Bai, H. Ade, R. Spontak, C. Balik, and C. Koch, "X-ray microscopy of novel thermoplastic/liquid crystalline polymer blends by mechanical alloying," *Macromolecules Rapid Communications*, vol. 19, pp. 557-561, 1998.

H. Zhang, G. R. Zhuang, H. Ade, C.-H. Ko, B. Winn, J. Kirz, D. Leta, R. Polizzotti, S. Cameron, S. Hulbert, and E. Johnson, "Recent progress with the scanning photoemission microscope at the national synchrotron light source," in Thieme et al. [186], pp. II-143-156.

